



HHS Public Access

Author manuscript

J Mol Biol. Author manuscript; available in PMC 2022 September 17.

Published in final edited form as:

J Mol Biol. 2021 September 17; 433(19): 167198. doi:10.1016/j.jmb.2021.167198.

A Novel Approach for the Synthesis of Human Heteropolymer Ferritins of Different H to L Subunit Ratios

Ayush K. Srivastava¹, Paolo Arosio², Maura Poli², Fadi Bou-Abdallah¹

¹ Department of Chemistry, State University of New York, Potsdam, NY 13676, USA

² Department of Molecular and Translational Medicine, University of Brescia, 25121 Brescia, Italy

Abstract

Mammalian ferritins are predominantly heteropolymeric species consisting of 24 structurally similar, but functionally different subunit types, named H and L, that co-assemble in different proportions. Despite their discovery more than 8 decades ago, recombinant human heteropolymer ferritins have never been synthesized, owing to the lack of a good expression system. Here, we describe for the first time a unique approach that uses a novel plasmid design that enables the synthesis of these complex ferritin nanostructures. Our study reveals an original system that can be easily tuned by altering the concentrations of two inducers, allowing the synthesis of a full spectrum of heteropolymer ferritins, from H-rich to L-rich ferritins and any combinations in-between (isoferritins). The H to L subunit composition of purified ferritin heteropolymers was analyzed by SDS-PAGE and capillary gel electrophoresis, and their iron handling properties characterized by light absorption spectroscopy. Our novel approach allows future investigations of the structural and functional differences of isoferritin populations, which remain largely obscure. This is particularly exciting since a change in the ferritin H- to L-subunit ratio could potentially lead to new iron core morphologies for various applications in bio-nanotechnologies.

Keywords

Iron oxidation; H-rich ferritin; L-rich ferritin; Isoferritin; Capillary gel electrophoresis

Introduction

Ferritin is a ubiquitous iron storage protein and a highly conserved supramolecular nanostructure that plays a key role in iron homeostasis.¹⁻⁷ By storing iron safely and

Correspondence to Fadi Bou-Abdallah: bouabdf@potsdam.edu (F. Bou-Abdallah).

CRedit authorship contribution statement

Ayush K. Srivastava: Conceptualization, Methodology, Investigation, Writing – original draft. **Paolo Arosio:** Conceptualization, Methodology, Investigation, Writing – review & editing, Supervision. **Maura Poli:** Conceptualization, Methodology, Supervision.

Fadi Bou-Abdallah: Conceptualization, Methodology, Investigation, Writing – review & editing, Supervision.

DECLARATION OF COMPETING INTEREST

The authors declare that they have no known competing financial interests or personal relationships that could have appeared to influence the work reported in this paper.

Appendix A. Supplementary material

Supplementary data to this article can be found online at <https://doi.org/10.1016/j.jmb.2021.167198>.

reversibly, ferritins overcome the problem of poor iron bioavailability and toxicity while providing an iron source for the synthesis of heme and iron-containing proteins.²⁻⁵ Human ferritin is composed of two subunit types, named H and L, which co-assemble in various proportions to form a shell-like protein nanostructure of 24 subunits (i.e. isoferritins) within which a mineralized iron core is deposited.²⁻⁵ The two subunits are encoded by distinct genes located on chromosome 11 (for the H-chain) and chromosome 19 (for the L-chain) and have different promoters,⁸ but the same posttranscriptional iron-dependent regulation,^{9,10} Different tissue types express ferritin with different proportion of the two subunits; for example, heart ferritins are rich in H-chains, while liver ferritins are rich in L-chains.²⁻⁵ The H-subunits have ferroxidase activity that are necessary for the removal of redox active ferrous ions in cells, owing to the rapid oxidation of Fe(II) ions and the subsequent formation of a stable inorganic Fe(III) core.¹¹⁻¹³ The L-subunits have iron nucleation centers that facilitate iron nucleation and mineralization inside the ferritin hollow cavity.²⁻⁵ All types of ferritins (i.e. homopolymer only H-subunits, homopolymer only L-subunits, and heteropolymer mixed H and L subunits) oxidize and store iron, albeit at different rates.^{1,14}

Although the in-vitro mechanism of Fe(II) oxidation and mineral core formation has been extensively investigated,^{1-7,11-14} it is still unclear how iron is loaded into the protein in-vivo.¹⁴ Similarly, in-vitro iron mobilization from ferritin can be achieved using a variety of reducing agents, but the in-vivo mechanism is not well understood.¹⁵ Although it is widely accepted that the major pathway of ferritin iron mobilization involves a lysosomal proteolytic degradation followed by dissolution of the iron mineral core, it is not clear whether auxiliary iron mobilization mechanisms involving physiological reducing agents, and/or cellular reductases, contribute to the release of iron from ferritin.^{14,15} Recent studies have shown that a specific mechanism of ferritin degradation via lysosomal autophagy (called ferritinophagy)¹⁶⁻¹⁹ involves the Nuclear Receptor Coactivator-4 (NCOA4). Under conditions of cellular iron depletion, NCOA4 binds to ferritin H-subunits, but not L-subunits, and carries the complex to autophagolysosomes for protein degradation and cellular iron recycling.¹⁵⁻¹⁹ Although ferritinophagy is thought to involve all types of ferritins (heteropolymer H-rich and L-rich ferritins), it is unclear how the lysosomal degradation of homopolymer L-chain ferritin, or heteropolymer L-rich ferritin occurs, given the high specificity of NCOA4 recognition by ferritin H-subunits.¹⁵

Notably, mechanistic studies of ferritins have been performed almost exclusively with recombinant human homopolymeric H-subunit or homopolymeric L-subunit proteins, with only a handful of studies conducted with H-rich or L-rich heteropolymers that mimic naturally occurring ferritins in-vivo.^{1,2,11-15,19} This is quite surprising given that the majority of natural ferritins found in human tissues are heteropolymers.^{3,5} One of the impediments to studying ferritin heteropolymers is an inherent difficulty in cloning, expressing, and producing heteropolymer H/L ferritins. Earlier *in-vitro* reconstitution attempts using chemical denaturation and unfolding of recombinant homopolymers H- and L-ferritins, followed by their renaturation, have largely failed, were irreproducible or unpredictable, or have yielded very low amounts of functional heteropolymer ferritins that are not representative of those occurring naturally.²⁰⁻²⁶ Nonetheless, the results of these studies have shown that heteropolymer ferritins have properties that differ significantly

from homopolymers.^{1,20-26} Thus, we thought to design a new ferritin expression system to produce recombinant heteropolymer ferritins with different H/L subunit ratios, mimicking those found in various organs and tissues, and then compare their iron uptake kinetics.

Recombinant ferritin is normally synthesized by transforming *E. coli* with vectors that express either subunits under a strong and inducible promoter. Typically, the 24-mer homopolymer H-ferritin is effectively expressed by pET vectors that have a T7 promoter, and by pASK vectors that have a Tet promoter. However, production of the 24-mer homopolymer L-ferritin is more complex, since when expressed under T7 promoters, it accumulates as an insoluble fraction in the *E. coli* extracts.²⁷ The homopolymer L-ferritin is usually expressed by vectors with a Trp promoter that is induced after the consumption of Trp in cells. Taking advantage of a pWUR 1 + 2 tetO mut89 vector²⁸ sold by Addgene (plasmid #80102), we engineered our own ferritin plasmid in which the cDNA of human ferritin H-subunit (FTH) is cloned downstream the T7 promoter (controlled by Lac I repressor and induced by IPTG), and the cDNA of human ferritin L-subunit (FTL) is cloned downstream the Tet-On system (controlled by tetO operator and induced by anhydrotetracycline, Tet). Our engineered plasmid (named pWUR-FtH-TetO-FtL) provides a unique opportunity to explore the structure–function of these protein nanostructures and their implications in iron homeostasis and various pathological conditions, and allows the design of novel iron core nanostructures and morphologies for a variety of applications.

Results

Ferritin expression in *E. coli* Rosetta-gami B strain

To explore the potential of the ferritin H- and L-subunits to co-assemble and form heteropolymeric species, we chose to work with a new and modified *E. coli* strain (i.e. Rosetta-gami B): Chromosomal Genotype: F⁻ ompT hsdSB (rB⁻ mB⁻) gal dcm lacY1 ahpC (DE3) gor522: Tn10 trxB pRARE (CamR, KanR, TetR). Rosetta-gami B carries a chromosomal copy of the T7 RNA polymerase gene under control of the lacUV5 promoter. However, the Rosetta-gami B strain carries a mutation in the lac permease (lacY) that allows a uniform and fast IPTG entry into cells, similar to that of Tetracycline, which is known to enter the cell by passive diffusion.²⁹ This mutation is expected to facilitate the regulation of protein expression levels with regard to the T7 promoter and IPTG concentration. We therefore transformed this strain of *E. coli* with pWUR-FtH-TetO-FtL plasmid and used different concentrations of IPTG and Tet for protein expression. As expected, very low concentrations of IPTG were needed for efficient protein expression (Figure 1). Several cell cultures were grown (20, 200 and 1000 mL) at 37 °C and 200-250 rpm agitation using different concentrations of IPTG (5–100 μM) and Tet (100–1000 ng/ml). As shown in Figure 1, one single sharp band, similar to that of H- and L-homopolymers appears on 7.5% native-PAGE, suggesting that the H- and L-subunits have co-assembled into one type of ferritin species. Additionally, the native-PAGE results showed slightly different band mobility of heteropolymer ferritins with the H-rich ferritins migrating further down on the gels compared to L-rich ferritins. To confirm that the ferritin species is an H/L heteropolymer, the samples were run on 12% SDS-PAGE (Figure 1) and revealed the presence of both types of subunits. More importantly, different concentrations of inducers

were shown to produce different types of heteropolymers with different H to L subunits composition (Figure 2).

Quantification of ferritin heteropolymer subunit composition with capillary gel electrophoresis (SDS-CGE)

To examine the integrity of the H- and L-subunits and quantify the ferritin heteropolymer subunit composition, capillary gel electrophoresis (CGE) was used under denaturing conditions (SDS-CGE). The SDS-CGE electropherograms of a few ferritin samples prepared under the same conditions of Figure 1 showed well-resolved peaks for the L-subunit and the H-subunit, with migration times of 17 min and 17.7 min, respectively. From the area under the CE peaks, the subunit composition of the various heteropolymer ferritins were calculated, with the inducers' conditions displayed next to each electropherogram (Figure 2(A)). These results matched those predicted from the gels band intensities of Figure 1. Table S1 displays a series of experimental conditions with expected (based on gel intensity) and confirmed (using SDS-CGE) H to L subunit ratios (on a percentage base) in different heteropolymer ferritin samples obtained under different IPTG and Tet concentrations, cell culture volume, and with or without 0.1% glucose. Figure 2(B) shows a plot of the number of H-subunits in ferritin heteropolymers as a function of IPTG and Tet concentrations, produced in 1L cell cultures in the presence of 0.1% glucose.

Iron oxidation kinetics in heteropolymer ferritins

UV-vis spectrophotometric kinetic measurements were conducted to evaluate the ability of H/L heteropolymer ferritin to oxidize Fe (II) and form a mineral core. Figure 3 shows an increase in absorbance at 305 nm (due to the formation of oxo/hydroxo Fe(III) species) following the addition of 500 Fe(II)/protein to six different ferritin samples with different H- to L-subunit ratio. The molar absorptivity value of the oxidized iron core is determined to be $3000 \pm 500 \text{ M}^{-1} \text{ cm}^{-1}$, in accord with published literature.^{1,2,11,12} The iron oxidation rates are displayed in Figure 3(B) and show that variations in the H to L subunit ratio have major effects on the functionality of ferritin heteropolymers. H-rich heteropolymer ferritins (i.e. H₂₃:L₁ and H₂₁:L₃) have about 10-fold higher Fe(II) oxidation rate than L-rich ferritins heteropolymer ferritins (i.e. H₁:L₂₃ and H₅:L₁₉), consistent with the rapid Fe(II) ferroxidase activity of H-subunits,^{1,2,30,31} whereas homopolymer H-ferritin (H₂₄) displayed ~ 40 times higher Fe(II) oxidation rates compared to homopolymer L-ferritin (L₂₄), which lacks ferroxidase activity.

Discussion

One major in-vitro property of ferritin is that it can reversibly denature in acidic or basic media to produce individual free subunits or monomers, which self-assemble to re-form the stable 24-mer shell at neutral pH. The kinetics of ferritin's self-assembly was found to depend on several factors including subunit concentration, pH, and ionic strength,³² and could take up to 10 min for the subunits to re-organize. Although the assembly process was studied under conditions far from physiological, the in-vivo cellular assembly of ferritin subunits may be completely different and may involve protein chaperones, other biomolecules or cellular components. Conversely, an earlier study found the pH-induced

apoferritin disassembly and reassembly processes were not fully reversible, and that the structural recovery of the 24-mer ferritin during pH-induced reassembly depended on the history of the disassembly process.³³

While the assembly process of ferritin subunits can be performed with homopolymer H-subunits or homopolymer L-subunits ferritin, a fluorescence resonance energy transfer (FRET) investigation²⁶ demonstrated the preferential formation of H/L hybrid heteropolymers, when both H- and L-subunits are present in the medium. However, the in-vivo mechanism of such assembly is still unclear and whether the 24-mer heteropolymeric structure is completely random or directed by specific subunit-subunit interactions remains unresolved. One alternative approach would be to design a novel plasmid that would allow for the overexpression and auto-assembly of ferritin heteropolymers in *E. coli*, similarly to naturally occurring ferritins in mammalian tissues. Using our engineered plasmid, in which the H- and L-subunits are under the influence of different promoters, we demonstrate our ability to produce heteropolymer isoferritins with different H:L subunit ratios. Our novel in-vivo ferritin production methodology yields ferritin samples that are a better representation of native ferritins present in mammalian tissues, compared to ferritins produced by the denaturation and renaturation procedure, allowing for the expression of any desired H to L subunit ratio covering the full spectrum of isoferritins, from H₂₄:L₀ to H₀:L₂₄ and anything in between.

Ferritin expression in the Rosetta gamie B host produced single bands on native PAGE and 2 distinct bands on SDS-PAGE, consistent with the formation of ferritin heteropolymers (Figure 1). Interestingly, when different inducer concentrations were used, we observed the formation of different ferritin heteropolymers with specific H to L ratios, suggesting that transformed Rosetta gamie cells can be easily tuned to produce essentially any desired heteropolymer ferritin structures with specific H and L subunits combination. Our CE results demonstrate the accurate quantification of ferritin subunits in any of our purified heteropolymers and was consistent with the predicted ratios of H and L subunits from native PAGE. To prove that our purified heteropolymer ferritins are fully functional, iron uptake and oxidation kinetics were performed and demonstrated that H-rich ferritins exhibit similar kinetics to those of the extensively studied homopolymer H-ferritin (Figure 3), with the rates of oxidation falling off dramatically as the ferritin H-content decreases. Changes in the H to L subunit ratio that occur during cellular proliferation or differentiation may therefore have a significant effect on the functionality of heteropolymers in tissues, with H-rich ferritins having fast iron incorporation rates suitable for active organs like heart and brain for efficient iron detoxification and cellular protection, whereas L-rich ferritins having much slower iron oxidation kinetics that are more suited for iron storage tissues such as livers and spleens.

Although very little is known about the driving forces that bring the H and L subunits together, and/or the complementary roles that these subunits play during iron uptake, oxidation, mineralization and/or mobilization, the mechanism of native heteropolymer ferritin nanostructure assembly has never been studied, mainly because of the lack of a good protein expression system. With our novel plasmid design, we are now able to synthesize these complex nanostructures, with high purity, allowing us to investigate in future studies

how specific arrangements of different H- to L-subunit ratios lead to different ferritin isomers with unique iron storage and release activities, and how these processes reflect the localization of isoferritins and ultimately their biological functions within tissues. We speculate that the non-linear dependence of the iron oxidation rates versus ferritin H-content (Figure 3) may reflect preferential interactions between H and L subunits to form dimers or multimer assembly, as previously suggested.^{20,26} Additionally, it has been proposed that the presence of the L-subunits disrupted the formation of H-H dimers²⁶ and that the H-subunits arrange themselves at distant positions on the heteropolymeric shell, up to at least eight subunits per ferritin molecule, beyond which they start to co-localize. These results are consistent with our kinetic studies which show a very low rates of iron oxidation in L-rich heteropolymers, up to a ratio of about 12H:12L, as noted by the break at around 50:50 H:L in Figure 3. As the number of H-subunits increases, a rapid and linear increase in the iron oxidation rates is observed until an H-content of ~90% is reached. The data also suggest that the presence of a few L-subunits on the heteropolymer (i.e. <3 L-subunits) exhibits no effect on the overall rate of iron oxidation.

Interestingly, the most dramatic change in the iron oxidation rates occurs between H21:L3 and H13:L11, accounting for almost 80% drop in iron oxidation activity. Even more dramatic, is the fact that the presence of 1 less H-subunit on the ferritin shell exhibited a 40 % drop in oxidative activity (i.e. H21:L3 vs. H20:L4), suggesting that the presence of a few L-subunits (i.e. 4 L-subunits) had a dramatic and a negative effect on the protein ferroxidase activity. Notably, an earlier study²⁰ showed that unfolded H and L human ferritin subunits renatured to form heteropolymers similar to native ones, and that the rates of iron oxidation linearly increased up to 30% content in H-subunits, beyond which no further increase in rates was observed even with an increasing H-subunits content, suggesting that a limited number of H subunits (i.e. 7 or 8 H-subunits) are needed for maximum rates of ferritin iron uptake. These early results do not agree with our current data and suggest that native or in-vivo produced heteropolymer ferritin may differ from those reconstituted in-vitro through a denaturation and a renaturation process, even though the individual subunits have apparently co-assembled to form a ferritin-like shell. Indeed, preliminary results suggest that the process of denaturing and refolding of ferritin causes protein oxidation, detected by MALDI-TOF in the form of an increase in the number of oxygen atoms on the protein. A recent study from our lab employing H-rich and L-rich heteropolymer ferritins (expressed in-vivo using bicistronic expression vectors) showed that H-rich ferritins (i.e. H20:L4) exhibited fast iron oxidation kinetics (i.e. average rate of 0.005 Abs/s compared to 0.007 Abs/s in this work), similarly to homopolymer H-ferritins (i.e. H24), and that L-rich ferritins have a very slow iron oxidation kinetics (10 to 15-fold slower, under conditions similar to our present work). These results are in keeping with the roles of L-rich ferritins in slow iron incorporation and storage, and of H-rich ferritins in minimizing iron-catalyzed production of reactive oxygen species, in tissues of high metabolic activity.

Surprisingly, despite the widespread occurrence of heteropolymer ferritins in tissues of vertebrates, very little is known about the complementary roles that H and L subunits play during iron uptake, iron mineralization and mobilization.^{1,14,15} Our new approach could therefore herald a dramatic acceleration in the design of novel ferritin heteropolymers, not only for structure–function characterization, but also to help facilitate exploitation of ferritin

as a nano-template for nano-chemistry and nanotechnology research. Current research in our lab is looking into the effect of H and L subunits on the rates of iron oxidation and core mineralization, but also on iron mobilization from ferritin. Additional avenues of research include investigating how specific arrangements of different H- to L-subunit ratios lead to different ferritin isomers with unique iron storage and release activities, and how these processes reflect the localization of isoferritins and ultimately their biological functions within tissues. This is particularly exciting since a change in the ferritin H- to L-subunit ratio could lead to new iron core nanostructures and morphologies for various applications in bio-nanotechnologies. Future studies with these newly synthesized heteropolymer ferritins may help address major questions in ferritin chemistry, help us better understand the role of ferritin in iron homeostasis, and its implication in various neurological and iron-related diseases.

Materials and Methods

Construction of the pWUR-FTH-tetO-FTL plasmid

A detailed description of the pWUR-FTH-tetO-FTL plasmid construction is provided in the supplementary information (Figure S1) along with a schematic of its map. To verify correct cloning, the DNA sequence of the plasmid was first analyzed on 1% agarose gel after restriction digestion at Xho1 and Hind III sites (Figure S2) and then confirmed by sequencing. Immunoblotting of ferritin H and L subunits stained with the H-subunit monoclonal antibody rH02 and L-subunit chain LF03 was also performed (Figure S3)

Cell transformation

The plasmid (10–20 ng DNA) was added to competent cells (Rosetta gamie B strain of *E. coli*) and placed on ice for 30 min. The mixture was heated at 42 °C for 90 s without shaking, followed by 2 min cooling on ice and then incubated in LB-medium at 37 °C for 1 h. Different amounts of this culture (e.g., 100 µL, 900 µL) were plated on LB spectinomycin agar plates and incubated overnight at 37 °C. A single colony was then selected for protein expression.

Ferritin expression and purification

Transformed cells were induced at 37 °C for 4 h using 10–1000 µM isopropyl β-D-1-thiogalactopyranoside (IPTG from Sigma-Aldrich), 25–1600 ng/ml of anhydrotetracycline (IBA Lifesciences GmbH). After centrifugation, the cell pellet was resuspended into 15 ml of 20 mM Tris-HCl pH 7.4, sonicated for 1 min using 3 cycles at 50–60% amplitude, and centrifuged for 10 min at 12,000 rpm. The supernatant was heated at 75 °C, incubated for 10–15 min, and then centrifuged for 20 min at 12,000 rpm. The supernatant was then analyzed for protein expression using 12% SDS-PAGE with Coomassie blue (Sigma-Aldrich) staining.

The supernatant was subjected to protein precipitation (5.3 g of ammonium sulfate added to 10 ml of supernatant and incubated overnight at 4 °C), followed by an overnight dialysis at 4 °C against 5 L of 20 mM Tris HCl, 1 mM NaN₃, pH 7.4. The dialyzed solution was centrifuged at 12,000 rpm for 20 min, to remove any precipitates, and further purified

using size exclusion chromatography (SEC) and a 10/600 column packed with Superdex 200 (Akta Go, GE Healthcare). The SEC column was initially equilibrated with 50 mM MOPS, 100 mM NaCl buffer pH 7.4, and the protein run was performed at a linear flow rate of 0.5 ml/min. The fractions with the highest purity of ferritin were collected and concentrated with 100 kDa cut-off centrifugal devices (Pall) at 4 °C using amicon air pressure concentrator. Protein quantification was performed with Micro BCA Protein Assay Kit (Thermo Scientific).

To determine ferritin speciation and sample homogeneity, we have tested several heteropolymer ferritin preparations following solution fractionation using Superdex 200 column chromatography, and then testing these fractions by SDS-CGE. Our results suggest about 10–15% ferritin heterogeneity in any given ferritin preparation using LB media from Sigma-Aldrich (i.e. an H19:L5 heteropolymer would be an average composition of heteropolymers having H and L subunit composition ranging between 18–20 H and 4–6 L).

Ferritin yields

The following average amounts have been obtained in 1 L cultures. Plasmid construct, yield, ferritin type:

- pET FTH, > 50 mg/L, human homopolymer H ferritin
- pASK FTH, 20–40 mg/L, human homopolymer H ferritin
- pDS20 FTL, 4–6 mg/L, human homopolymer L ferritin
- pASK FtL-FTH, 10 mg/L, H-rich 70 %H:30 %L human heteropolymer ferritin
- pWUR FTH-tetO-FTL, 10–15 mg/L, all types of human heteropolymer ferritins (this work). This average yield of purified human heteropolymer ferritins using the pWUR plasmid was about the same, irrespective of the type of ferritin or the H to L subunit ratio.

Capillary gel electrophoresis (SDS-CGE)

To quantify the integrity and the H- and L-subunit composition of purified recombinant human heteropolymer ferritins, capillary gel electrophoresis (CGE) was used under denaturing conditions (SDS-CGE). The reagents of the Sciex CE-SDS analysis kit include SDS-MW gel buffer (proprietary formulation, pH 8, 0.2% SDS), CE-SDS sample buffer (100 mM Tris-HCl pH 9.0, 1% SDS), acidic wash solution (0.1 N HCl), and basic wash solution (0.1 N NaOH). An Agilent Technologies 50 mm ID bare fused silica capillary, with a total length of 33 cm and an effective length 24.5 cm was used in the SDS-CGE experiments. The SDS-CGE capillary was pre-conditioned under a high pressure of 2.0 bar using 0.1 N NaOH (10 min), 0.1 N HCl (5 min), water (2 min), and finally a high-pressure flush (4.0 bar) of the SDS gel buffer for 10 min. Prior to each protein run, the capillary was conditioned under a high pressure flush of 4 bar using 0.1 N NaOH (3 min), 0.1 N HCl (1 min), water (1 min) and finally SDS gel buffer (10 min). The protein samples were injected electro-kinetically by applying a negative voltage of –5 kV for 20 s. Protein subunits separation was followed under a negative applied voltage of –16.5 kV for 30 min. A 2.0 bar pressure was applied to both inlet and outlet vials for the duration of the experiment with the

capillary temperature maintained at 25.00 °C. The detection wavelength was set at 220 nm (10 nm bandwidth) with a 350 nm reference wavelength (10 nm bandwidth) and a response time of 1 s. Typically, ferritin solutions (100 µL at 1–2 mg/ml) were prepared in an SDS sample buffer (>60% by volume) in the presence of 5 µL 2-beta-mercaptoethanol (5% v/v) from Sigma-Aldrich. The ferritin solution was mixed thoroughly, tightly capped and heated in a 100 °C water bath for at least 10 min. The protein solution was then cooled to room temperature prior to running on the 7100-model capillary electrophoresis instrument from Agilent Technologies.

Densitometric analysis

For a semi-quantitation of band intensity, the SDS-PAGE of human recombinant ferritins were first imaged on a Kodak digital science image station 440CF. Analysis of band intensity was performed using Kodak 1D image analysis software (v. 3.6.3) or the NIH ImageJ software (Figure S4). Once the lanes and bands were identified and framed, the intensity of each band was estimated by the software after background subtraction of a lane without added protein.

Immunoblotting

Purified human ferritin (1 µg) was loaded onto 7.5% native PAGE and transferred to Hybond-P Membrane (GE) using a semi-dry western blot technique. The primary antibody for the immunoblotting assay was the mouse monoclonal rH02 for human H-chain and the monoclonal LF03 for the human L-chain. After incubation with horseradish peroxidase-conjugated secondary antibody, membranes were developed with Super Signal West Pico Chemiluminescent Substrate (Thermo Scientific-Pierce) and visualized with LI-COR (Odyssey).

Fe(II) oxidation kinetics

Conventional UV–vis spectroscopy was performed on a Varian Cary 50 Bio (or Cary 60) spectrophotometers from Agilent Technologies. All iron oxidation kinetics in ferritin were conducted at 25.00 °C in 100 mM MOPS buffer, 100 mM NaCl, pH 7.4 using freshly prepared samples using independent protein preparations to ensure reproducibility. The kinetic traces were followed at 305 nm where the Fe(III) oxo(hydroxo) species absorbs. The instrument was zeroed using the “iron-free” ferritin solution, prepared in buffer as the blank. We note that in our studies, “iron-free” ferritins refer to purified ferritin samples, as expressed in *E. coli*, without any treatment to remove residual iron, which under our experimental conditions were found to contain ~50–75 Fe(III) ions per protein. Typically, for the iron oxidation kinetics, 2–3 µL of a ferrous sulfate solution prepared in deionized H₂O (pH 2.0) were injected into a 1.0 ml protein solution containing a spin bar for rapid mixing. Other experimental conditions are stated in the figure captions.

Supplementary Material

Refer to Web version on PubMed Central for supplementary material.

Funding

This work is supported by a National Science Foundation, Division of Molecular and Cellular Biosciences (MCB) Award 1934666, the Camille & Henry Dreyfus Foundation, Inc., The Henry Dreyfus Teacher-Scholar Award (Award TH-16-007), a Cottrell Instrumentation Supplements Award from the Research Corporation for Science Advancement (Award #27452), and the National Institute of Health Grant R15GM104879.

References

1. Mehlenbacher M, Poli M, Arosio P, Santambrogio P, Levi S, Chasteen ND, Bou-Abdallah F, (2017). Iron oxidation and core formation in recombinant heteropolymeric human ferritins. *Biochemistry*, 56, 3900–3912. [PubMed: 28636371]
2. Bou-Abdallah F, (2010). The iron redox and hydrolysis chemistry of the ferritins. *Biochim. Biophys. Acta (BBA)-General Subj*, 1800, 719–731.
3. Harrison PM, Arosio P, (1996). The ferritins: molecular properties, iron storage function and cellular regulation. *Biochim. Biophys. Acta (BBA)-Bioenerg*, 1275, 161–203.
4. Chasteen ND, Harrison PM, (1999). Mineralization in ferritin: an efficient means of iron storage. *J. Struct. Biol*, 126, 182–194. [PubMed: 10441528]
5. Arosio P, Ingrassia R, Cavadini P, (2009). Ferritins: a family of molecules for iron storage, antioxidation and more. *Biochim. Biophys. Acta, Gen. Subj*, 1790, 589–599.
6. Theil EC, Tosha T, Behera RK, (2016). Solving biology's iron chemistry problem with ferritin protein nanocages. *Acc. Chem. Res*, 49, 784–791. [PubMed: 27136423]
7. Theil EC, (2013). Ferritin: the protein nanocage and iron biomineral in health and in disease. *Inorg. Chem*, 52, 12223–12233. [PubMed: 24102308]
8. Worwood Met al., (1985). Assignment of human ferritin genes to chromosomes 11 and 19q13.3→19qter. *Hum. Genet*, 69, 371–374. [PubMed: 3857215]
9. Torti FM, Torti SV, (2002). Regulation of ferritin genes and protein. *Blood*, 99, 3505–3516. [PubMed: 11986201]
10. Dario Finazzi D, Arosio P, (2014). Biology of ferritin in mammals: an update on iron storage, oxidative damage and neurodegeneration. *Arch. Toxicol*, 88, 1787–1802. [PubMed: 25119494]
11. Bou-Abdallah F, Zhao G, Mayne HR, Arosio P, Chasteen ND, (2005). Origin of the unusual kinetics of iron deposition in human H-chain ferritin. *J. Am. Chem. Soc*, 127, 3885–3893. [PubMed: 15771525]
12. Bou-Abdallah F, Zhao G, Biasiotto G, Poli M, Arosio P, Chasteen ND, (2008). Facilitated diffusion of iron(II) and dioxygen substrates into human H-chain ferritin. A fluorescence and absorbance study employing the ferroxidase center substitution Y34W. *J. Am. Chem. Soc*, 130, 17801–17811. [PubMed: 19055359]
13. Bou-Abdallah F, Flint N, Wilkinson T, Salim S, Srivastava AK, Poli M, Arosio P, Melman A, (2019). Ferritin exhibits Michaelis-Menten behavior with oxygen but not with iron during iron oxidation and core mineralization. *Metallomics*, 11, 774–783. [PubMed: 30720039]
14. Melman A, Bou-Abdallah F, (2020). Iron mineralization and core dissociation in mammalian homopolymeric H-ferritin: Current understanding and future perspectives. *Biochim. Biophys. Acta, Gen. Subj*, 1864, 129700 [PubMed: 32798636]
15. Bou-Abdallah F, Paliakkara JJ, Melman G, Melman A, (2018). Reductive mobilization of iron from intact ferritin: mechanisms and physiological implication. *Pharmaceuticals*, 11, 120.
16. Mancias JD, Wang X, Gygi SP, Harper JW, Kimmelman AC, (2014). Quantitative proteomics identifies NCOA4 as the cargo receptor mediating ferritinophagy. *Nature*, 508, 105–109.
17. Santana-Codina N, Mancias JD, (2018). The role of NCOA4-mediated ferritinophagy in health and disease. *Pharmaceuticals*, 11, 114.
18. Gryzik M, Srivastava A, Longhi G, Bertuzzi M, Gianoncelli A, Carmona F, Poli M, Arosio P, (2017). Expression and characterization of the ferritin binding domain of Nuclear Receptor Coactivator-4 (NCOA4). *Biochim. Biophys. Acta (BBA)-General Subj*, 1861, 2710–2716.

19. Srivastava AK, Flint H, Kreckel M, Gryzik M, Poli M, Arosio P, Bou-Abdallah F, (2020). Thermodynamic and kinetic studies of the nuclear receptor coactivator- 4 (NCOA4) interaction with human ferritin. *Biochemistry*, 29, 2707–2717.
20. Santambrogio P, Levi S, Cozzi A, Rovida E, Albertini A, Arosio P, (1993). Production and characterization of recombinant heteropolymers of human ferritin H and L chains. *J. Biol. Chem*, 268, 12744–12748. [PubMed: 8509409]
21. Levi S, Santambrogio P, Cozzi A, Rovida E, Corsi B, Tamborini E, Spada A, Albertini A, Arosio P, (1994). The role of the L-chain in ferritin iron incorporation. Studies of homo and heteropolymers. *J. Mol. Biol*, 238, 649–654. [PubMed: 8182740]
22. Kim HJ, Kim HM, Kim JH, Ryu KS, Park SM, Jahng KY, Yang MS, Kim DH, (2003). Expression of heteropolymeric ferritin improves iron storage in *Saccharomyces cerevisiae*. *Appl. Environ. Microbiol*, 69, 1999–2005. [PubMed: 12676675]
23. Rucker P, Torti FM, Torti SV, (1997). Recombinant ferritin: modulation of subunit stoichiometry in bacterial expression system. *Protein Eng., Des. Sel*, 10, 967–973.
24. Lee J, Seo HY, Jeon ES, Park OS, Lee KM, Park CU, Kim KS, (2001). Cooperative activity of subunits of human ferritin heteropolymers in *Escherichia coli*. *Biochem. Mol. Biol*, 34, 365–370.
25. Masuda T, Goto F, Yoshihara T, Ezure T, Suzuki T, Kobayashi S, Shikata M, Utsumi S, (2007). Construction of homo- and heteropolymers of plant ferritin subunits using an in-vitro protein expression system. *Protein Expression Purif.*, 56, 237–246.
26. Carmona F, Poli P, Bertuzzi M, Gianoncelli A, Gangemi F, Arosio P, (2017). Study of ferritin self-assembly and heteropolymer formation by the use of Fluorescence Resonance Energy Transfer (FRET) technology. *Biochim. Biophys. Acta, Gen. Subj*, 1861, 522–532. [PubMed: 27993659]
27. Santambrogio P, Cozzi A, Levi S, Rovida E, Magni F, Albertini A, Arosio P, (2000). Functional and immunological analysis of recombinant mouse H- and L-ferritins from *Escherichia coli*. *Protein Expression Purif.*, 19, 212–218.
28. Shipman Seth L., Nivala Jeff, Macklis Jeffrey D., Church George M., (2016). Molecular recordings by directed CRISPR spacer acquisition. *Science*, 353aaf1175. [PubMed: 27284167]
29. Orth P, Schnappinger D, Hillen W, Saenger W, Hinrichst W, (2000). Structural basis of gene regulation by the tetracycline inducible Tet repressor-operator system. *Nat. Struct. Biol*, 7, 215–219. [PubMed: 10700280]
30. Zhao G, Bou-Abdallah F, Arosio P, Levi S, Janus-Chandler C, Chasteen ND, (2003). Multiple pathways for mineral core formation in mammalian apoferritin. The role of hydrogen peroxide. *Biochemistry*, 42, 3142–3150. [PubMed: 12627982]
31. Zhao G, Bou-Abdallah F, Yang X, Arosio P, Chasteen ND, (2001). Is hydrogen peroxide produced during iron (II) oxidation in mammalian apoferritins? *Biochemistry*, 40, 10832–10838. [PubMed: 11535059]
32. Mohanty A, Mithra K, Jena SS, Behera RK, (2021). Kinetics of ferritin self-assembly by laser light scattering: impact of subunit concentration, pH, and Ionic strength. *Biomacromolecules*, 22, 1389–1398. [PubMed: 33720694]
33. Kim M, Rho Y, Jin KS, Ahn B, Jung S, Kim H, Ree M, (2011). pH-dependent structures of ferritin and apoferritin in solution: disassembly and reassembly. *Biomacromolecules*, 12, 1629–1640. [PubMed: 21446722]

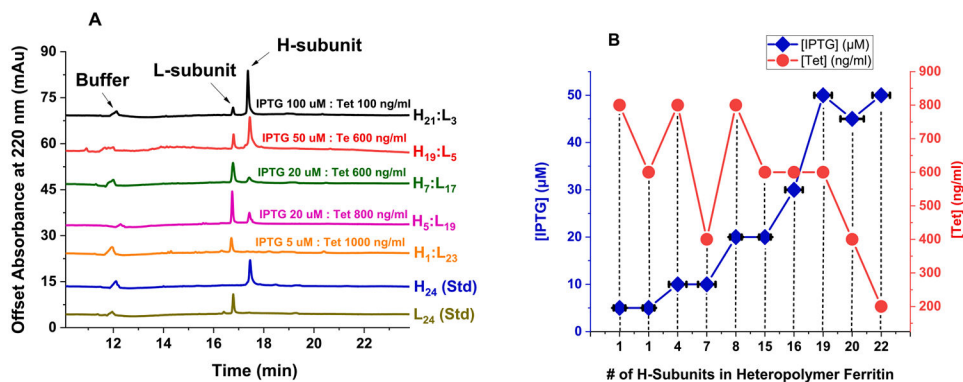


Figure 2. (A) Representative SDS-CGE electropherograms of recombinant human H/L heteropolymer ferritin samples produced in Figure 1. Typical protein concentrations ranged from 1 to 2 mg/ml. The instrument conditions are specified under Materials and Methods. (B) Plot of the number of H-subunits in ferritin heteropolymers as a function of IPTG and Tet concentrations, purified from 1 L cell cultures using LB media from Sigma-Aldrich, in the presence of 0.1% glucose.. Error bars along the x-axis represent average variations in the H-subunits content of heteropolymer ferritins.

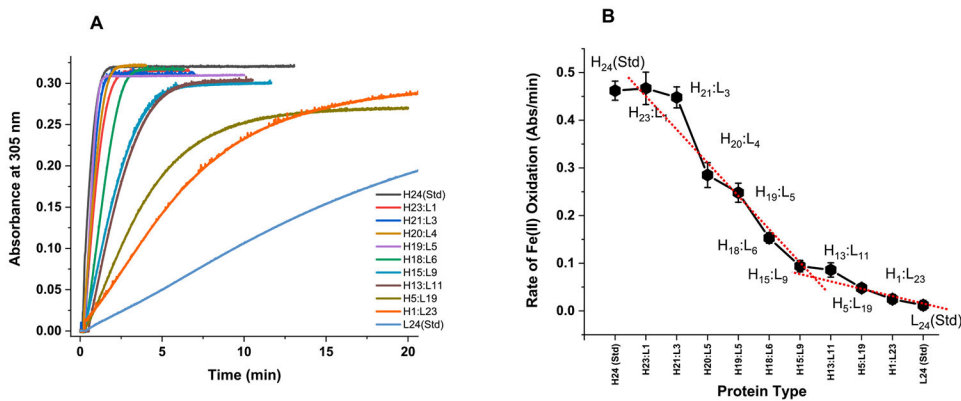


Figure 3. Iron oxidation kinetics in ferritin at 305 nm using light absorption spectroscopy. The kinetic curves in (A) represent the formation of ferritin Fe(III) core following the addition of 500 Fe(II) ions to ferritin. The Fe(II) oxidation rates in (B) are derived from the kinetic data in (A) for the first minute of the reaction. Conditions: 0.2 μ M ferritin in 100 mM Mops, 100 mM NaCl, 100 μ M FeSO₄, pH 7.4, 25.00 °C. The red dotted line is a linear fit to the data and shows a break at ~50:50 H:L ratio.